Studies on the Plane Turbulent Wall Jet

By Takashi SAITO*, Hirofumi OHNARI** and Nobuyoshi AKASHI***

(Received July 15, 1978)

Abstract

As for wall jet, the pioneering investigation was done by Glauert[1] and the appealing work has been performed by Schwartz[2] and Cosart and Tsuchiya[5]. In these investigation, smooth wall was chosen as the subject, and analysis was done assuming the similarity of the velocity distribution. On a practical case of hydraulic engineering, it may be to consider that the wall was rough hydraulically. In such a case, the boundary layer growth is closely related to the scale of roughness. Therefore, with the above assumption, a theory of this problem can't be developed. As all studies show that the law of the wall is not applciable to the turbulent wall jet in the form that was obtained by experimentation in turbulent boundary layer, and turbulent pipe and channel flows. But we can't give a clear physical interpretation for it.

In this paper the author describe an experimental study of the characteristics of the plane turbulent wall jet issuing along smooth or rough boundary, and examine the distribution of the turbulent shear stress and the eddy viscous coefficient using the equation of motion applied the boundary layer approximation and the measured velocity distribution, and analyzed the boundary layer using these results. In consideration on the law of the wall, the boundary layer are divided into two regions, the first region is called the outer layer occupies the major portion of the flow, where the turbulence of the main flow plays an important role, second region is the wall region consists of viscous sublayer and turbulent sublayer, where the flow are defined by the property of the wall. The derived velocity law, in particular case, coincide with Parandtl-Kármán's logarithmic distribution, and contain the eddy viscosity coefficient of the main flow in position of parameter.

1. Introduction

The wall jet, named by Glauert[1] in 1656, is the flow with the velocity profile contacting at the maximum velocity points between two parts of the flow; one part is the boundary layer developing along the wall surface and another is the main flow with the same as the velocity profiles of a plane wall jet.

Also theoretical studies of the wall jet were first done by Glauert[1]. He analyzed with the Blasius law, assuming similarity solutions of velocity profiles in the boundary layer flow and main flow.

Glauert's pioneering achievements is high estimated, but subsequently some questions were pointed of the friction law by Schwartz and Tsuchiya et al.. Schwartz[2] made the experiment further in detail. Further more assuming the similarity solutions about the velocity profiles, he investigated the similarity about the velocity profiles and

* Department of civil engineering
** Tokuyama Technical College
*** Nishinippon Institute of Technology

the friction laws with the aid of the ordinal boundary layer similarity. As the results, he showed that the velocity profiles in the boundary layer were given as a power law having an exponent of 1/14, considering that the friction laws in the ordinal turbulent boundary layer can't be used to that in the wall jet. Tsuchiya[5] also gave the approximation of a law of 1/12 based on his experiments and proposed empirical equations which have greater coefficients of the wall surface friction than that in the Blasius law.

In many studies involved the above, the similarity law of the velocity profiles are applicable to the main flow part. Further more, it is common to all that the spread angle of the wall jet is smaller than that of the free jet, the velocity profiles in the boundary layer are uniformer than that of the ordinal turbulent boundary layer and the friction laws of the ordinal turbulent boundary layer is not applicable to that of the wall jet. But the physical interpretation of those characteristics have not been definite.

According to the calculation by Schwartz[2] and the experimental results by Eskinazi[7] and Kruka[8], the Reynolds stress profiles are recognized to be approximately the straight profiles as those of the open channel flow. Another speaking, the velocity profiles of the turbulent boundary layer in the wall jet are uniformer than those of the ordinal turbulent boundary layer. So this implies that eddy viscosities of the boundary layer in the wall jet are larger than those in the open channel flow. The physical meaning of this is supposed that the turbulence in the main flow where the scales of the mean flow and the turbulent flow are larger than those of the ordinal boundary layer flow, diffuse within the boundary layer. From describing the above, considering the velocity profiles and the friction law of the boundary layer in the wall jet, effects of the main flow to the boundary layer must be reflected.

Also characteristics of the wall jet on the rough bed must be clarified in the case of investigating the problems of the local scour and the criterion of the scour. But studies on the rough wall have been hardly examined except of the experimental studies on the submerged hydraulic jump by Kapaeva[4] and Rajaratnam[6].

We reports the results of the detailed experimental on the wall jet developing along the rough and smooth bed and clarifies the friction law and the velocity profiles law in the boundary layer and the characteristics of the wall jet.

As was stated above, to estimate the influence of the turbulence of the main flow in the boundary layer, we consider the boundary layer as constituting the wall surface range governed by the wall roughness and the outer layer influenced by the turbulence of the main flow. Further more we suppose that the flow of the wall surface range follows the results by Kurihara and the flow of the outer layer follows the derived law of the velocity profiles of assuming the eddy viscosity distributions. That is such distributions that coincide with the eddy viscosity of the main flow on the basis of the eddy viscosity distribution obtained by the reverse calculation with the aid of the motion equation applied the similarity of the boundary layer and the measured velocity profiles. This law of the velocity profile contains the parameter of the eddy viscosity in the main flow. We show that the calculated results by the supposed law

of the velocity profile agree well with experimental values, viz., the boundary layer growth, the skin friction coefficient, etc..

Lastly we show the applicable limits of the wall jet from the results of the systematic experiment on the effect of the downstream. It is practically very significant to grasp the applicable limits in the infinite depth, for the real current depth downstream of the sluice is finite.

2. Experimental apparatus and ways

Fig. 1 shows the experimental apparatus which is put together with steel frame and acrylic glasses. The width of that is 20 cm. The jet generator apparatus is fixed at the upstream side, which is made of the vinyl chloride pipes with the diameter of 20 cm. We used the acrylic glassed as the smooth bed. The wall roughness is adjusted to paste the sands on the bed, which have the uniform grain size as shown in Fig. 2. We adopted the 50% particle diameter as the characteristic of roughness.

For the measurement of velocity in the main flow, we used a pitot tube which were made of a stainless pipe with the inside diameter of 1.9 mm and the outside diameter

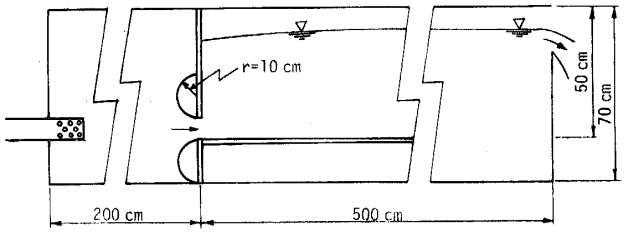

Fig. 1 Experimental apparatus.

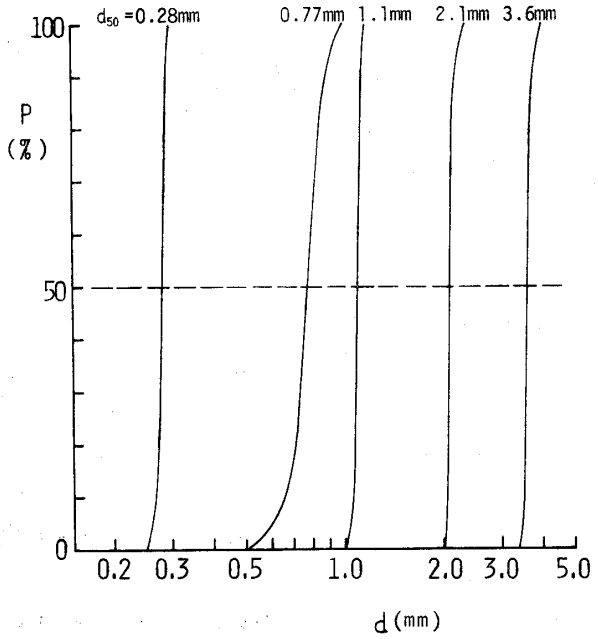

Fig. 2 Sands used in the experiments.

of 2.2 mm. For that in the boundary layer, we used a pitot tube which were manufactured the tip of the stainless pipe to the flat section with the thickness of 0.2 mm and the width of 4 mm.

3. Consideration of the experimental results

The experiment were done in the range of the nozzle thickness B_0 of 1.0 cm$\sim$ 1.54 cm and at a nozzle velocity of 80$\sim$400 cm/sec. The longitudinal velocity is measured in the range 10 cm$<x<$70 cm at intervals of 10 cm.

The definition sketch of the wall jet and the main symbols used in this paper is shown in Fig. 3. We named the range in which the maximum velocity is constant the zone of flow establishment and the range in which the flow is perfectly turbulent the zone of established flow as the same in the free jet.

The following is the description about the experimental results of the velocity profiles, the width of the main flow, the decay of the maximum velocity and the boundary layer growth.

1) The velocity profiles in the zone of established flow

The velocity profiles, which are demonstrated dimensionless with the maximum velocity U_m and the width of the flow $(\delta_0+\delta_B)$ as the characteristic velocity and length, are shown in Fig. 4. In the smooth surface the similarity of the velocity profile holds at the whole flow field except the condition of $x/B_0=10$. But the similarity in the rough surface does not hold good because the boundary layer thickness is large. x denotes the distance from the nozzle.

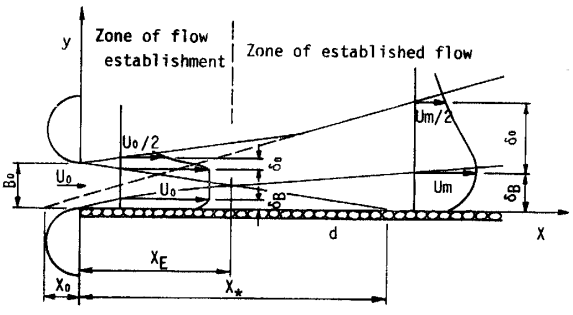

Fig. 3 Definition sketch of plane turbulent wall jet.

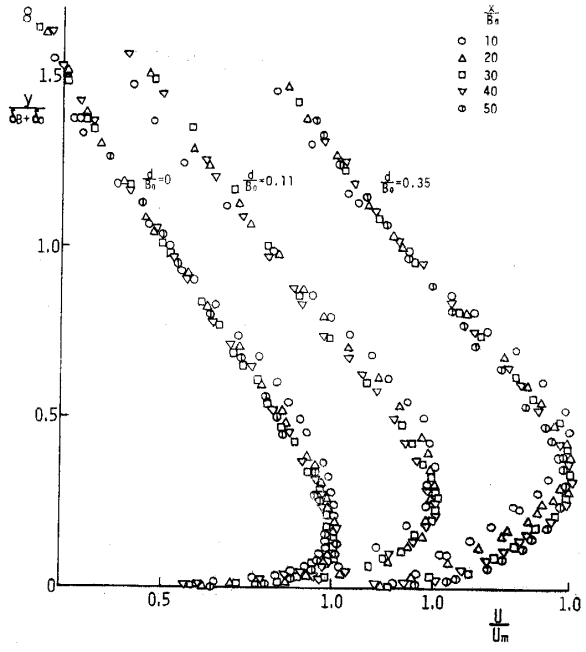

Fig. 4 Velocity profiles in a zone of established flow.

Considering the growth of the zone of established flow δ_0, we put in the virtual origin x_0 in the Görtler's solution about the free jet.

$$\frac{U}{U_m}=\operatorname{sech}^2\left(\sigma\frac{y-\delta_B}{x+x_0}\right) \qquad \cdots\cdots\cdots(1)$$

; when $y=\delta_B+\delta_0$, $U/U_m=0.5$. Consequently the following equation is directly obtained.

$$\frac{\delta_0}{B_0}=\frac{\cosh^{-1}\sqrt{2}}{\sigma}\left(\frac{x+x_0}{B_0}\right) \qquad \cdots\cdots\cdots(2)$$

Rewriting (2) with (1), we get:

$$\frac{U}{U_m}=\operatorname{sech}^2\left(\cosh^{-1}\sqrt{2}\cdot\frac{y-\delta_B}{\delta_0}\right) \qquad \cdots\cdots\cdots(3)$$

Fig. 5 shows the comparison between the experimental results and the above equation. The velocity profile in the main flow are approximately the same as that in the free jet, although the top of that profile come to a point slightly.

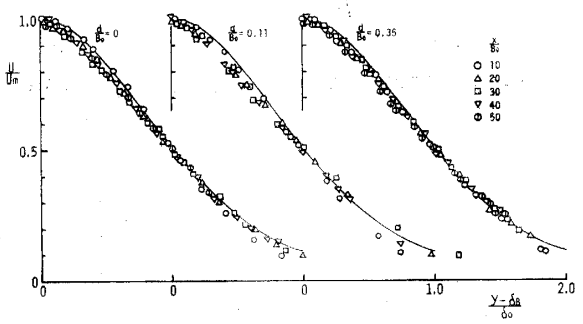

Fig. 5 velocity profiles in a main flow of the wall jet.

Now we try to compare the velocity distributions in the boundary layer at different sections in a dimensionless form. We plot U/U_m against y/δ_B. Fig. 6 (a, b, and c) illustrates this aspect with the linear scale and Fig. 6 (d, e, and f) with the double-logarithmic scale. The broken line with one points in Fig. 6–a is the mean velocity curve measured by Kruka and the line in Fig. 6–d is by a power law having exponents of 1/7, 1/12 and 1/14. The velocity profiles in the boundary layer are similarized by Tsuchiya for the 1/12 power law on the experimental result in the range of $x/B_0=9.3\sim35.0$ and for the 1/14 power law on that in the range of $x/B_0=24\sim60$ by Schwartz. From the experimental results in the range of $x/B_0=46\sim275$ by Kruka and $x/B_0=10\sim60$ by us, the velocity profiles in the boundary layer are founded that they have uniformer profiles as x/B_0 become to be greater. This intendancy is more clear as d/B_0 is larger, if the velocity profiles are with the variation of x/B_0. This treatment is very difficult.

Fig. 7 illustrates the ratio δ_B/δ_0 against x/B_0. From the experimental result on

the smooth bed, we get $\delta_B/\delta_0 \fallingdotseq 0.17(\delta_B/(\delta_0+\delta_B) \fallingdotseq 0.145)$ in the range of $x/B_0 > 20$. Approximately the above empirical equation agrees with the experimental results which were obtained. The changes of δ_B/δ_0 against x/B_0 on the roughed become to be large as the roughness d/B_0 become to be large.

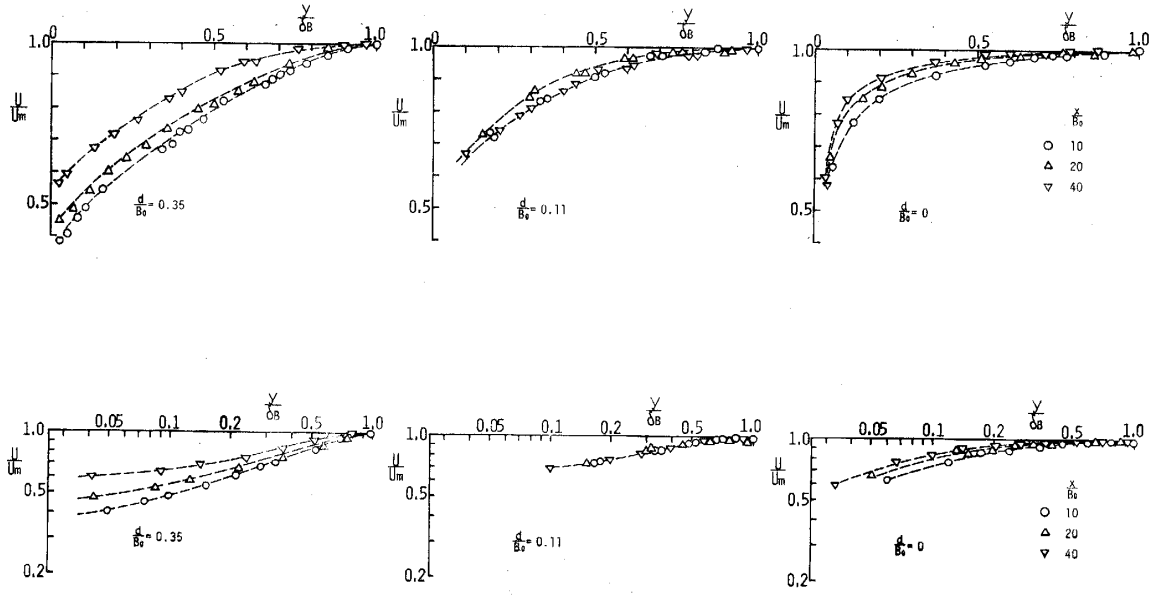

Fig. 6 Velocity profiles in boundary layers of the wall jet.

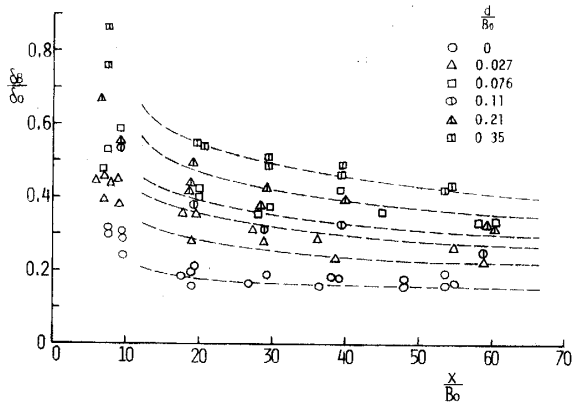

Fig. 7 Relative variation of characteristic length between the main flow and the boundary layer flow.

2) The growth of length scale in the main flow

The growth of length scale δ_0/B_0 in the zone of established flow is illustrated against x/B_0 in Fig. 8. The following empirical equation is shown as the straight line in that figure.

$$\frac{\delta_0}{B_0} = 0.068\left(\frac{x}{B_0} + 5.0\right) \qquad \cdots\cdots\cdots(4)$$

Approximately our experimental results agree with ever conclusions by many

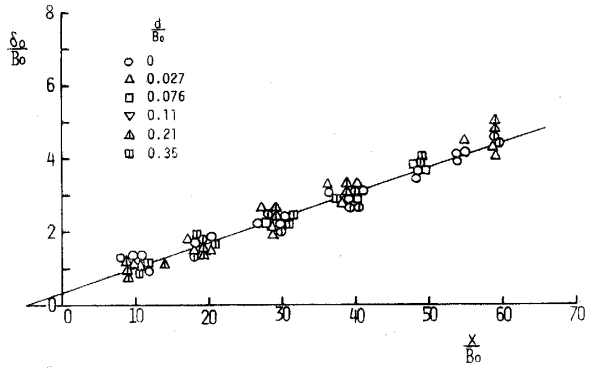

Fig. 8 Growth of the length scale in plane wall jets.

Table 1. Difusion coefficient in the main flow and the wall jet.

	Jet	Wall	$d\delta_0/dx$	σ	c
Albertson	Free	—	0.127	6.93	0.0388
Sigalla	Wall	Smooth	0.065	13.56	0.0142
Tsuchiya	〃	〃	0.059	15.03	0.0121
Schwart	〃	〃	0.068	12.96	0.0152
Kruka	〃	〃	0.060	14.67	0.0126
Saitou	〃	S & R	0.068	12.96	0.0152

investigators as Table 1, although the growth of the wall jet is smaller than that of the free jet. Comparing (2) with (4), we get:

$$\frac{x_0}{B_0}=5.0, \quad \sigma=\frac{\cosh^{-1}\sqrt{2}}{0.068}=12.96 \qquad \cdots\cdots\cdots(5)$$

whereas $\sigma=7.67$ (by Reichardt) in the free jet.

The growth gradient is shown according to the Tollmien's solution on the free jet as follows:

$$\frac{d\delta_0}{dx} \propto \left(\frac{l}{x}\right)^{2/3} \qquad \cdots\cdots\cdots(6)$$

where l is a mixing length.

Now supposing very simply that the main flow in the wall jet is the flow dividing the free jet into two at the maximum velocity point and the mixing length in the main flow is half of that in the free jet, the ratio of the growth gradient is $(0.5)^{2/3}=0.630$ from the eqn. (6). Considering that the values of the gradient in the free jet are $0.115\sim0.127$, the growth of the wall jet are $d\delta_0/dx=0.072\sim0.080$. Consequently we say that the growth of the wall jet is similar to that of the free jet. From this conclusion and the consideration of the velocity profile, it is conjectured that the main flow of the wall jet have a nearly constant mixing length at each section as same as the free jet.

3) The decay of the maximum velocity and the potential core length

Applying the law of the momentum conservation for the main flow, where the boundary layer is neglected, and using the eqn. (1) of the velocity profile the decay of the maximum velocity is described by the following eqn.;

$$\frac{U_m}{U_0}=\sqrt{\frac{3\sigma}{2}\Big/\frac{x+x_0}{B_0}} \qquad \cdots\cdots\cdots(7)$$

Putting $U_m/U_0=1$ into (7), the imaginary point x_* in Fig. 3 is obtained as follows;

$$\frac{x_*}{B_0}=\frac{3}{2}\sigma-\frac{x_0}{B_0}=14.44 \qquad \cdots\cdots\cdots(8)$$

Assuming that the gradient consuming the potential core and this gradient does not vary with the boundary layer growth, we can seek for the shifting points from the zone of flow establishment to the zone of established flow. The flows in the neighborhood of the maximum velocity outside of the boundary layer have the property of the potential flow and the constant maximum velocity, and so the boundary layer growth is similar to that of the ordinal boundary layer.

In the zone of flow establishment, applying the Blasius law to the flow on the smooth surface and the formula of Manning-Strickler to the flow on the rough surface, the growth of the boundary layer is described by the eqn.;

$$\left.\begin{aligned}\frac{\delta_B}{x}&=0.37\left(\frac{\nu}{U_0x}\right)^{1/5} \quad \text{for Smooth}\\ \frac{\delta_B}{x}&=0.248\left(\frac{k_s}{x}\right)^{1/4} \quad \text{for Rough}\end{aligned}\right\} \qquad \cdots\cdots\cdots(9)$$

Now let's take δ_{BE} as the boundary layer thickness at the x_E point. From the geometrical relation in Fig. 3, $\delta_{BE}/B_0=1-x_E/x_*$. So, when we know the relation δ_{BE} and x_E from the eqn. (9), we get the shifting point x_E to the zone of established flow;

$$\left.\begin{aligned}\frac{x_E}{B_0}\Big/\left\{1-0.37\,\frac{x_E}{U_0}\left(\frac{\nu}{U_0x_E}\right)^{1/5}\right\}&=\frac{x_*}{B_0} \quad \text{for Smooth}\\ \frac{x_E}{B_0}\Big/\left\{1-0.248\,\frac{x_E}{B_0}\left(\frac{k_s}{x_E}\right)^{1/4}\right\}&=\frac{x_*}{B_0} \quad \text{for Rough}\end{aligned}\right\} \qquad \cdots\cdots\cdots(10)$$

where k_s is the equivalent roughness and ν is the kinetic viscosity coefficient. Under the condition of $U_m/U_0=1$ at $x=x_E$, rewriting the eqn. (7), we get;

$$\frac{U_m}{U_0}=\sqrt{\frac{x_E+x_0}{x+x_0}} \qquad \cdots\cdots\cdots(11)$$

Fig. 9 illustrates the comparison of the experimental results with the calculated results by the eqns. (10), (11). Experimental values agree well with the calculated results. We conclude that the formula of momentum conservation can be applied for

the main flow. Investigating the momentum issued from the nozzle by the eqns. (1), (11), we recognized that the momentum decreased with the boundary layer growth in the zone of flow establishment.

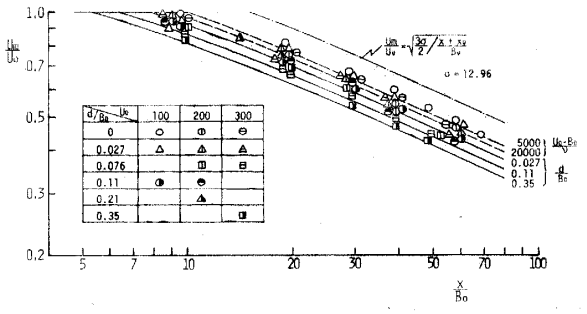

Fig. 9 Decay of maximum velocity in plane wall jets.

4) The growth of the boundary layer

It is known that the friction law under the ordinal boundary layer can't be applied to the wall jet. Here we investigate whether the friction law of the same form as that of the turbulent boundary layer which has been ever used can be applied to the wall jet boundary layer.

Rewriting the boundary layer momentum equation for the incompressible steady flow with the displacement thickness δ_*, the momentum thickness θ and the shear velocity U_*, by neglecting the term of the pressure dp/dx as same as the treatment by Tsuchiya, Schwartz et al., (we describe empirically the condition to be unable to neglect lately), we get the following equations.

$$\left(\frac{U_*}{U_m}\right)^2=\frac{d\theta}{dx}+\frac{\delta_B}{U_m}\left(2\frac{\theta}{\delta_B}+\frac{\delta_*}{\delta_B}-1\right)\frac{dU_m}{dx} \qquad \cdots\cdots\cdots(12)$$

$$\delta_*=\int_0^{\delta_B}\left(1-\frac{U}{U_m}\right)dy,\quad \theta=\int_0^{\delta_B}\frac{U}{U_m}\left(1-\frac{U}{U_m}\right)dy$$

Adopting the velocity profile of the boundary layer with the logarithmic profile and the decay of the maximum velocity with the eqn. (11), we calculated the boundary layer growth by using the above equation. Fig. 10 illustrates the comparison between the experimental results and the calculated results. Also the results calculated with the Blasius law and the formula of Manning-Strickler is almost similar as the results with the logarithmic law. Comparing the experimental results with the calculated, we find that the calculated is comparatively lower than the experimental results.

We considered that the following to investigate these results. First, we supposed the velocity profile in the boundary layer is given with the power form:

$$\left.\begin{aligned}&\frac{U}{U_m}=\left(\frac{y}{\delta_B}\right)^n\\&\left(\frac{U_*}{U_m}\right)^2=\frac{1}{2}C_x=\gamma\left(\frac{U_m\cdot\delta_B}{\nu}\right)^{-2n/(n+1)}\end{aligned}\right\} \qquad \cdots\cdots\cdots(13)$$

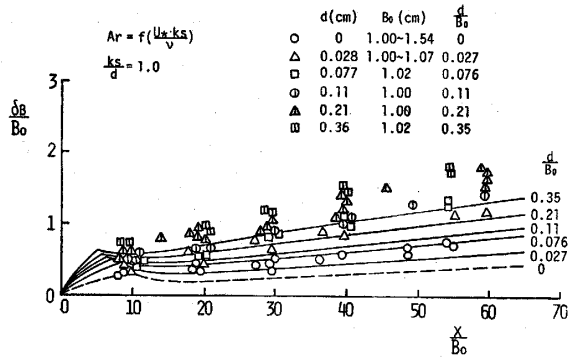

Fig. 10 Boundary layer groth in plane wall jets.

When we seek for the values of n and γ in such a way that the measured boundary layer thickness coincide with the calculated by the above eqn. at each section, the relation of n and γ can be shown in Fig. 11. If curve of $n \sim \gamma$ for all of x/B_0 intersect each other at one point, they are decided to be constant values. But they can't be settled as shown in this figure, secondarily in the same way as the above, assuming the velocity profiles with the logarithmic form as following;

$$\frac{U}{U_*} = A_r\left(\frac{U_* \cdot k_s}{\nu}\right) + \frac{1}{\kappa} \ln \frac{y}{k_s} \qquad \cdots\cdots\cdots(14)$$

We show the values of A_r and k_s/B_0 to agree the measured with the calculated in Fig. 12. If the values of A_r and k_s/B_0 in that figure is used, the calculation of boundary layer growth is possible. But we can't interpret of the physical means to such values.

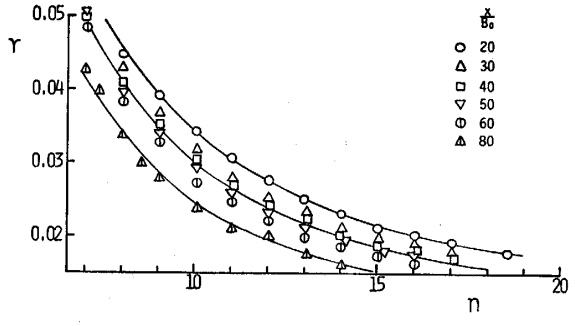

Fig. 11 Corelation of n and γ (n is exponents of power laws and γ is coefficients of friction laws)

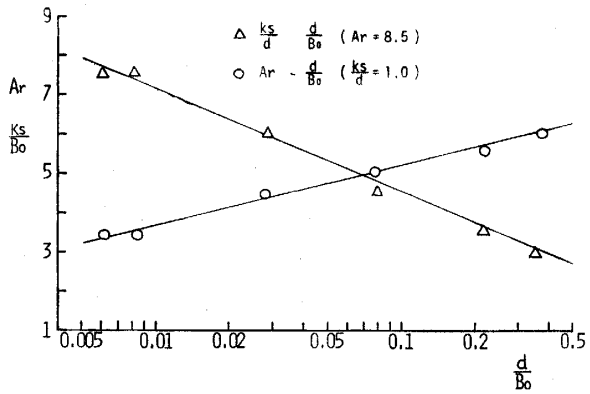

Fig. 12 Corelation of A_R with K_s/B_0 under the logarithmic laws.

4. Theoretical consideration on the friction law

As was described before, we recognized that the friction law of the ordinal turbulent boundary layer can't be applied to the wall jet. It can be considered that the distributions of the eddy viscosity in the turbulent boundary layer of the wall jet is

very different from that in the ordinal turbulent boundary layer.

We examine qualitatively the eddy viscosity, because the quantitative examination is difficult, particularly in the neighborhood of $du/dy \fallingdotseq 0$, and consider the friction law, dividing the flow according to the mean characteristic of the boundary layer.

1) The shear stress distribution and the eddy viscosity coefficient

Rewriting the equation of the motion applied the ordinal boundary layer similarity with the continuity equation, we get;

$$U\frac{\partial u}{\partial x}-\int_0^y \frac{\partial u}{\partial x}dy\cdot\frac{\partial u}{\partial y}+\frac{\partial \overline{u'v'}}{\partial y}=\nu\frac{\partial^2 u}{\partial y^2} \qquad \cdots\cdots\cdots(15)$$

where u', v' is the turbulent fluctuating velocities in the x-, y-coordinate directions. As v/u in the main flow have the order of $d\delta_0/dx$, the boundary layer similarity can be also applied to the main flow.

For the all section in the wall jet, we introduce a distribution function of the velocity and the Reynolds stress as following:

$$\left.\begin{aligned}&\frac{U}{U_m}=f\left(\zeta,\frac{x}{B_0}\right),\quad \frac{\overline{u'v'}}{U_m^2}=g\left(\zeta,\frac{x}{B_0}\right)\\&\zeta=\frac{y}{\delta},\quad \delta=\delta_0+\delta_B\end{aligned}\right\} \qquad \cdots\cdots\cdots(16)$$

, $\overline{u'v'}$ approach to be 0 when the value of ζ become to have the infinite value. So, by substituting (16) into (15) and integrating from ζ to the infinity, we obtain:

$$g(\zeta, x/B_0)=\left(2\frac{\delta}{U_m}\frac{dU_m}{dx}+\frac{d\delta}{dx}\right)\int_\zeta^\infty f^2 d\zeta+\left(\frac{\delta}{U_m}\frac{dU_m}{dx}+\frac{d\delta}{dx}\right)f\int_0^\zeta f d\zeta$$
$$+\frac{\nu}{U_m\delta}\frac{\partial f}{\partial\zeta}+\delta\frac{\partial}{\partial x}\int_\zeta^\infty f^2 d\zeta-\delta f\frac{\partial}{\partial x}\int_0^\zeta f d\zeta \qquad \cdots\cdots\cdots(17)$$

The third term in right hand side have a important role in the extreme neighborhood of the wall surface. But in the most of the flow, that can be neglected as the minute term. Further more we neglect also the fourth and fifth terms as the change of the velocity profile for x/B_0 is small. Substituting the experimental equation (4), (9) into (17), we get;

$$\frac{g(\zeta, x/B_0)}{\beta(1+m)}=\left(1-\frac{x+x_0'}{x+x_0}\right)\int_\zeta^\infty f^2 d\zeta+\left(1-\frac{1}{2}\frac{x+x_0'}{x+x_0}\right)f\int_0^\zeta f d\zeta \qquad \cdots\cdots\cdots(18)$$

where x_0' denotes the virtual origin in the eqn. (4): $x_0'/B_0=5.0$. x_0 denotes the virtual origin in the eqn. (9): $x_0/B_0=\sigma/3=4.32$, $\beta=d\delta_0/dx=0.068$, $m=\delta_B/\delta_0=F(x/B_0)$. We supposed that the shear stress τ_0 at the wall surface is demonstrated as $\tau_0/\rho=-U_m^2 g(0, x/B_0)$, the following equation is obtained;

$$\frac{\tau_0}{\rho U_m^2}=-\beta(1+m)\left(1-\frac{x+x_0'}{x+x_0}\right)\int_0^\infty f^2 d\zeta \qquad \cdots\cdots\cdots(19)$$

Consequently the distributions of the shear stress and the eddy viscosity coefficient is obtained from the above two eqns..

$$\frac{\tau}{\tau_0} = -\left\{\left(1-\frac{x+x_0'}{x+x_0}\right)\int_\zeta^\infty f^2 d\zeta + \left(1-\frac{1}{2}\frac{x+x_0'}{x+x_0}\right) f\int_0^\zeta f d\zeta\right\} \Big/ \left\{\left(1-\frac{x+x_0'}{x+x_0}\right)\int_0^\infty f^2 d\zeta\right\} \quad \cdots\cdots(20)$$

$$\frac{\varepsilon}{U_m \delta_0} = -\frac{g(\zeta, x/B_0)}{f'(\zeta, x/B_0)} \quad \cdots\cdots(21)$$

When m is given as a broken line in Fig. 7 and the measured velocity distribution is given at each section of the flow, the results calculated by the eqns. (20), (21) is illustrated in Fig. 13. For the comparison with the results which were ever obtained, the shear stress distribution measured by Eskinazi et al.[7),8)] and calculated by Schwartz et al.[2)] is shown in Fig. 13.

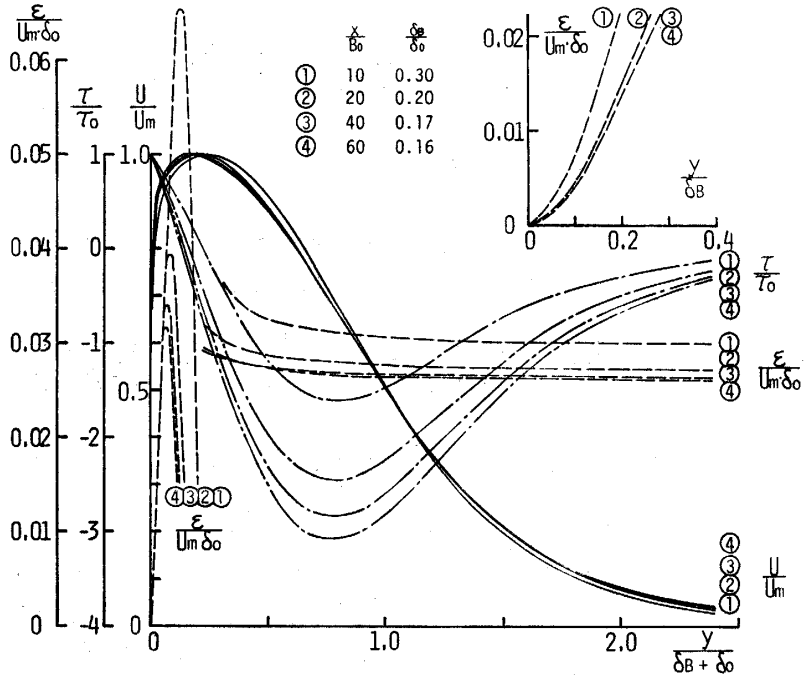

Fig. 13 Distributions of shear stress and eddy viscosity coefficient in plane wall jets along the smooth wall.

From the observation of the calculated results of the eddy viscosity coefficient, we find that the fluctuation are extremely heavy near the maximum velocity. But this fluctuations make no great sense for the velocity gradient. We illustrated to magnify the calculated results that the velocity gradient is comparatively great. The increasing rate of the eddy viscosity coefficient near the wall become to be great as that of the main flow become to be great. This may be estimated to be right, considering the continuity of eddy viscosity. Calculating the eddy viscosity coefficient from the ex-

perimental results by Reichardt and the Gortler's solution[10], $\varepsilon/U_m\delta_0$ get 0.037. In Fig. 13, that in the main flow of the wall jet along the smooth wall have the values of $0.03\sim0.026$. Those values are slightly small owing to the influence of the wall which has already discussed. Table 2 represents the results on which we examined the influence of the boundary layer velocity profile and the ratio δ_B/δ_0 of the flow scale to the eddy viscosity of the main flow. The eddy viscosity coefficient at a half maximum velocity points are not affected almostly by the exponent of the power law. From the table, we find that the eddy viscosity coefficient are not hardly influence by the difference in the boundary layer velocity profile and the eddy viscosity coefficient increases as m increases.

Table 3 represents the eddy viscosity coefficient under the rough wall at the point of $x/B_0=40$ and half of the maximum velocity.

Table 2. Changes of eddy viscosity coefficient with and velocity profiles in boundary layer of wall jet.

m \ α_1	1/4	1/8	1/12	1/16	1/20
0.15	0.0252	0.0256	0.0257	0.0258	0.0258
0.20	275	280	282	283	283
0.25	298	305	307	309	309
0.30	323	331	334	336	337
0.35	348	358	362	364	365
0.40	375	386	391	393	395
0.45	402	416	421	423	425
0.50	431	446	452	455	457

Table 3. Eddy viscosity coefficient in the main flow of plane wall jets.

d/B_0	δ_m/δ_0	$\varepsilon/Um\delta_0$	$\varepsilon/U_0\sigma_0$
0.35	0.455	0.0424	0.0088
0.21	0.390	385	83
0.11	0.330	358	77
0.076	0.300	334	75
0.027	0.240	287	68
0	0.160	262	67

2) The law of velocity profile in boundary layer

On the condition that a wall surface is finely smooth, there is a viscous sublayer in which a kinematic eddy viscosity does not effect on the flow mechanism along the wall surface. Similarly, on condition that a wall are rough, a extreme thin sublayer

in which the fluid viscosity plays an important role should exist along rough surface. Therefore, it can be taken into consideration the existence of an apparent viscosity sublayer which have an average constant thickness along the bed wall surface.

M. Kurihara[16] explained the turbulent flow fields of two types, which are named vortextype and wake-type and caused by the wall surface roughness, occurred in the neighborhood of the roughness wall. In consequence, the turbulent sublayer which indicates the hydraulic characteristics of a roughness can be introduced between the viscous sublayer and the inner layer which predominates the major parts of the flow.

As was stated above, in average, a boundary layer can be classified three layers which are a viscous sublayer, a turbulent sublayer and an inner layer, and then, let's consider the laws of velocity profile of those layers respectively.

Strictly speaking, a shear stress distribution in boundary layer does not indicate a linear distribution in the effect of the action of inertial forces, but under the calculation described above and the experimental report by Kuruka, it is possible to be considered that the shear stress distribution curve is linear in this case practically. So an equation of shear stress is assumed as follow,

$$\frac{\tau}{\rho}=\frac{\tau_0}{\rho}=(1-\eta)=U_*^2(1-\eta),\quad \eta=\frac{y}{\delta_B} \qquad \cdots\cdots\cdots(22)$$

where τ_0 denotes a shear stress of the wall surface.

Both values of the kinematic eddy viscosity in main flow and boundary layer should be same at the boundary section respectively, and considering the stated characteristics of those distribution, a kinematic eddy viscosity in boundary layer will be assumed as follows,

$$\varepsilon=\kappa U^*\delta_B\eta(1-E\eta),\quad E=1-\frac{\alpha U_m\delta_0}{\kappa U_*\delta_B} \qquad \cdots\cdots\cdots(23)$$

in where, α denotes a non-dimensional kinematic eddy viscosity in main flow, which distribution is homogeneous, in Table 3.

In the steady flow of an incompressible fluid, if we neglect the term of an inertial force which is very small, Eulerian equation of motion which was applicated of the boundary layer approximation can be written in the following for.

$$\frac{\tau}{\rho}=\nu\frac{dU}{dy}-\overline{U'v'}=(\nu+\varepsilon)\frac{dU}{dy} \qquad \cdots\cdots\cdots(24)$$

Therefore, only considering of a fluid viscosity in a viscous sublayer, by integrating equation (24), the velocity distribution in a viscous sublayer is given as follows.

$$\frac{U}{U_*}=\frac{U_*y}{\nu}=\frac{1}{\kappa}R_*\eta,\quad R^*=\kappa\frac{U_*\delta_B}{\nu} \qquad \cdots\cdots\cdots(25)$$

Now we assume that the distribution of a kinematic eddy viscosity is homogeneous in turbulent sublayer, in which turbulent are owing to the wall surface and this sublayer itself is extremely thin as stated by Kurihara. Then we can obtain the following equa-

tion for velocity profile from eq. (24),

$$\frac{U}{U_*}=\frac{U_*\delta_B}{\nu}\left(1+\frac{\varepsilon}{\nu}\right)^{-1}\eta+C_1 \qquad \cdots\cdots\cdots(26)$$

in where, C_1 denote an integral constant.

By integrating eq. (24) introduced eqs. (22), (23), the equation for the velocity profile in the inner layer is given as follows.

$$\frac{U}{U_*}=\frac{1}{2\kappa E}\left\{\ln|ER_*\eta^2-R_*\eta-1|+\frac{R_*(1-2E)}{\sqrt{R_*^2+4ER_*}}\ln\left|\frac{2ER_*\eta-(R_*+\sqrt{R_*^2+4ER_*})}{2ER_*\eta-(R_*-\sqrt{R_*^2+4ER_*})}\cdot\frac{R_*-\sqrt{R_*^2+4ER_*}}{R_*+\sqrt{R_*^2+4ER_*}}\right|\right\}+C_2 \qquad \cdots\cdots\cdots(27)$$

in where, C_2 denote an integral constant.

Let η_1 and η_2 denotes the depths of the viscous sublayer and the turbulent sublayer. So we should transpose from η into eqs. (26), (27) to $(\eta-\eta_1)$. Furthermore, as both values of kinematic eddy viscosity in the inner layer and the turbulent sublayer should be same at the interface of each other, the kinematic eddy viscosity in the turbulent sublayer is given as follows.

$$\begin{aligned}\frac{\varepsilon}{\nu}&=\kappa\frac{U_*\delta_B}{\nu}(\eta_2-\eta_1)\{1-E(\eta_2-\eta_1)\}\\&=R_*(\eta_2-\eta_1)\{1-E(\eta_2-\eta_1)\}\end{aligned} \qquad \cdots\cdots\cdots(28)$$

By connecting the velocity at the interface of each layers, we shall be able to obtain the equations for the velocity profile in the turbulent sublayer and the inner layer respectively as follows.

$$\frac{U}{U_*}=\frac{1}{\kappa}\left[R_*\eta_1+\frac{R_*(\eta-\eta_1)}{1+R_*(\eta_2-\eta_1)\{1-E(\eta_2-\eta_1)\}}\right] \quad \text{for} \quad \eta_1>\eta>\eta_2 \cdots\cdots\cdots(29)$$

$$\begin{aligned}\frac{U}{U_*}=\frac{1}{\kappa}\Bigg[&R_*\eta_1+\frac{R_*(\eta_2-\eta_1)}{1+R_*(\eta_2-\eta_1)\{1-E(\eta_2-\eta_1)\}}\\&+\frac{1}{2E}\left\{\ln\left|\frac{ER_*(\eta-\eta_1)^2-R_*(\eta-\eta_1)-1}{ER_*(\eta_2-\eta_1)-R_*(\eta_2-\eta_1)-1}\right|\right.\\&\left.+\frac{R_*(1-2E)}{\sqrt{R_*^2+4ER_*}}\cdot\ln\left|\frac{2ER_*(\eta-\eta_1)-(R_*+\sqrt{R_*^2+4ER_*})}{2ER_*(\eta-\eta_1)-(R_*-\sqrt{R_*^2+3ER_*})}\cdot\right.\right.\\&\left.\left.\frac{2ER_*(\eta_2-\eta_1)-(R_*+\sqrt{R_*^2+4ER_*})}{2ER_*(\eta_2-\eta_1)-(R_*+\sqrt{R_*^2+4ER_*})}\right|\right\}\Bigg]\end{aligned} \qquad \cdots\cdots\cdots(30)$$

Kurihara[20] indicated the following equation on the thickness of the turbulent

sublayer from the consideration that it was almostly kept the condition which the occurrence and the dissipation of turbulent energy in the turbulent sublayer was an equilibrium.

$$\eta_2-\eta_1=\frac{k_s}{\delta_B}\left\{1-\exp\left(-0.055\left(\frac{U_* k_s}{\nu}-3.3\right)\right)\right\} \quad \cdots\cdots\cdots(31)$$

Let the thickness of the viscous sublayer search for on the smooth surface. The simplification of eq. (30) can be made by thinking of the case that R_* is sufficiently large and η is comparatively large on the condition $E=1$.

$$\frac{U}{U_*}=\frac{1}{\kappa}\{R_*\eta_1+\ln(R_*\eta)\} \quad \cdots\cdots\cdots(32)$$

The experimental results by Nikuradse in the smooth range is given as follows.

$$\frac{U}{U_*}=5.5+\frac{1}{\kappa}\ln\frac{U_* y}{\nu} \quad \cdots\cdots\cdots(33)$$

From comparison of eq. (32) and eq. (33), $\kappa=0.4$ and $U^* y_1/\nu=7.79$ are given.

With the same way on the case of smooth surface wall, the velocity profile in the inner layer on the rough wall was simplified as follows.

$$\frac{U}{U_*}=\frac{1}{\kappa}\left[R_*\eta_1+\frac{R_*(\eta_2-\eta_1)}{1+R_*(\eta_2-\eta_1)-R_*(\eta_2-\eta_1)^2}+\ln\frac{\eta}{\eta_2-\eta_1}\right]. \quad \cdots\cdots\cdots(34)$$

The experimental results by Nikuradse in the rough range are given as follows.

$$\frac{U}{U_*}=A_r+\frac{1}{\kappa}\ln\frac{y}{k_s}$$

$$A_r=8.5+0.744\left(\frac{U_* k_s}{\nu}-3.3\right)^{1/2}\cdot\exp\left\{-0.077\left(\frac{U_* k_s}{\nu}-3.3\right)\right\} \quad \cdots\cdots\cdots(35)$$

Comparison of eq. (35) and experimental results are shown in Fig. 14.

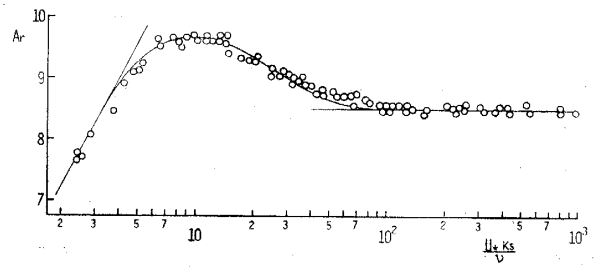

Fig. 14 Corelation of A_R and $U_* k_s/\nu$.

Comparing eq. (34) with eq. (35), $\kappa=0.4$ and the following equation is given.

$$\frac{U_* y_1}{\nu}=A_r+\frac{1}{\kappa}\left[\ln\left(\frac{k_s/\delta_B}{\eta_2-\eta_1}\right)-\frac{R_*(\eta_2-1)}{1+R_*(\eta_2-\eta_1)-R_*(\eta_2-\eta_1)^2}\right] \quad \cdots\cdots\cdots(36)$$

The calculation results of eq. (36) are shown in Fig. 16(a). This figure shows that the larger values of the relative roughness k_s/δ_B is the smaller thickness of the viscous sublayer $U_* y_1/\nu$. But the calculation results of the case that $U_* k_s/\nu$ is comparatively small can not be put confidence by the reason that R_* is enough large in the process to introduce eq. (36). Fig. 16(c) shows the difference of the thickness of the viscous sublayer on various relative roughness.

Fig. 15 shows the comparison the velocity distribution given by the calculation of eqs. (25), (30), when $E=1$ (with respect to ordinary boundary layer) and $\eta_2-\eta_1=0$

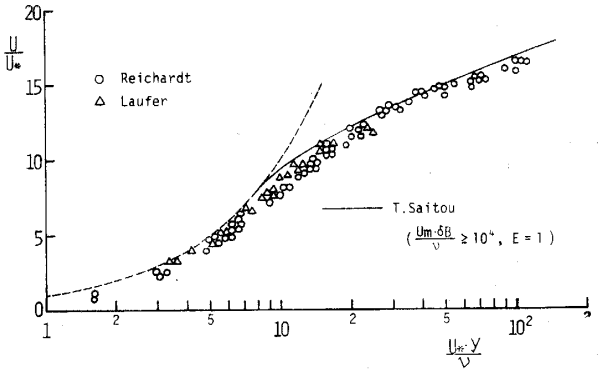

Fig. 15 Velocity protile of boundary layen along the Smooth wall.

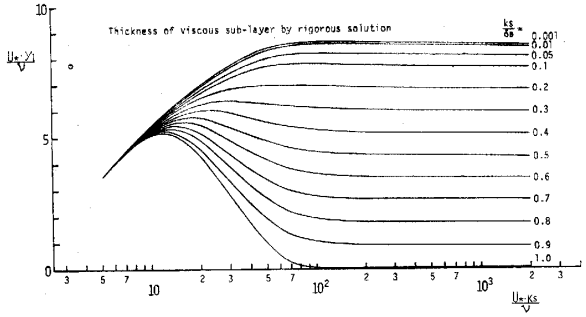

Fig. 16(a)

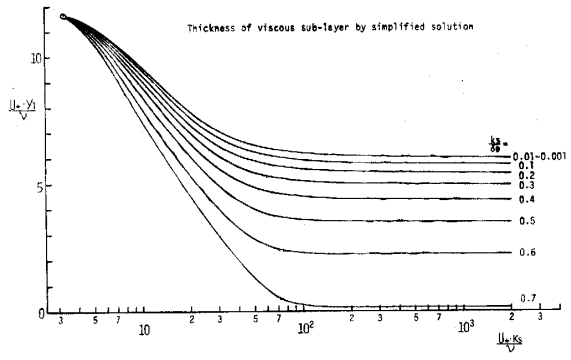

Fig. 16(b)

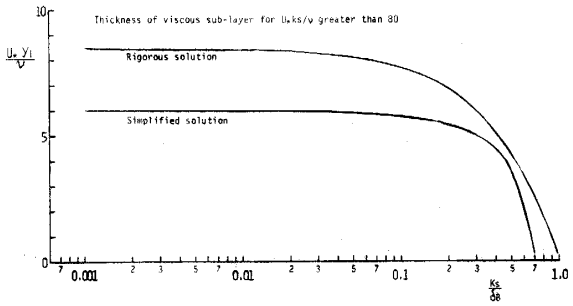

Fig. 16(c)

Fig. 16 Thickness of Viscous sublayer.

(on the smooth surface wall), with the measurements by Laufer (in pipe flow) and Reichardt (in open channel flow). There is very fine agreement with both results.

A simplified solution: Let make eq. (30) simple as this equation is complex, and if we use this equation to calculate for the growth of boundary layer, we shall need too many times and efforts.

Let introduce η_s to consist with a kinematic eddy viscosity and a fluid viscosity as the correction to take account of both fluid viscosity in the turbulent sublayer and the inner layer by reason of occurring a contraction that $(\nu+\varepsilon)$ is zero at the point of $\eta=\eta_1$, when we change η to $(\eta-\eta_1)$.

$$\kappa\frac{U_*\delta_B}{\nu}(\eta_1-\eta_2)\{1-E(\eta_1-\eta_2)\}=1 \qquad \cdots\cdots\cdots(37)$$

With the same way when the strictly solution are introduced, neglecting the fluid viscosity in eq. (24)*, the velocity profiles in the turbulent sublayer and the inner layer are given as follows.

$$\frac{U}{U_*}=\frac{1}{\kappa}\left[R_*\eta_1+\frac{\eta-\eta_1}{(\eta_2-\eta_s)\{1-E(\eta_2-\eta_s)\}}\right] \qquad \cdots\cdots\cdots(38)$$

$$\frac{U}{U_*}=\frac{1}{\kappa}\left[R_*\eta_1+\frac{\eta_2-\eta_1}{(\eta_2-\eta_s)\{1-E(\eta_2-\eta_s)\}}+\ln\left|\frac{\eta-\eta_s}{\eta_2-\eta_s}\right|+\frac{1-E}{E}\ln\left|\frac{1-E(\eta-\eta_s)}{1-E(\eta_2-\eta_s)}\right|\right] \qquad \cdots\cdots\cdots(39)$$

Fig. 16(b), (c) show the thickness of the viscous sublayer which are derived by comparing eqs. (33), (35) with eqs. (38), (39) at $E=1$.

Practical equation: Eq. (39) is considerably complex. Therefore, as same as Prandtl-Karman introduced, when we don't think of the complex flows near the wall surface, from the expedient boundary condition $U=0$ at $y=y_0$ and the kinematic eddy viscosity of eq. (23), the velocity distribution equation in boundary layer is given as follows.

$$\frac{U}{U_*}=\frac{1-E}{\kappa E}\ln\left|\frac{1-E\eta}{1-E\eta_0}\right|+\frac{1}{\kappa}\ln\frac{\eta}{\eta_0} \qquad \cdots\cdots\cdots(40)$$

In eq. (40), the first term of the right hand is a correction term owing to the turbulent action of the main flow, and at $E=1$, this equation consist with the low-law by Prandtl-Karman. Therefore we can adopt the same values of the expedient heights from surface, which were already used.

5. The growth of the boundary layer in the wall jet

In the zone of flow establishment ($x\leq x_E$), it can be consider that the velocity profile

* Now η equals $(\eta-\eta_s)$ though η equals $(\eta-\eta_1)$ in the strictly solution.

in boundary layer is same as that of an ordinary turbulent boundary layer. On the other hand, on the downstream enough, the velocity profile which was derived in Chap. 4 are performed. There is the transition regime from the zone of flow establishment to the zone of established flow, in where the velocity profile are not clarified. Now, if we assume that the diffusion of main flow turbulence equal to those of the free turbulent diffusion, it will be consider that the transition regime are the domain of (x^*-x_E). In this zone, it is possible to consider that the changes of velocity profile are indicated with the ratio of diffusion of main flow turbulence into the boundary layer, and to assume that the values of kinematic eddy viscosity of main flow, by which the velocity profile are determined, are given as follows.

$$\varepsilon=\alpha U_m\delta_0\frac{x-x_E}{x_*-x_E} \qquad \text{for} \quad x_E<x<x_* \qquad \cdots\cdots\cdots(41)$$

in where, α is given in Table 3, x_E and x^* are given by eqs. (11), (19) respectively.

The calculation of boundary layer growth are performed by eq. (10) from the jet entrance point to x_E, and by eqs. (30), (39), (40) at downstream of x_E for the velocity profile. The calculated results which were obtained in the way described above are shown in Fig. 17. In this figure, the calculated curves is in satisfactory agreement with the experimental results.

The calculated curves and experimental results on the local resistant coefficient are shown in Fig. 18. The experimental values are determined from the average gradient of velocity distribution which was illustrated on semi-log scale at an extent of η from 0.1 to 0.5 and eq. (39).

Fig. 19 shows the calculated curves and experimental results on the velocity profile in boundary layer. If we consider an error to determine the point of $dU/dy=0$, calculated results is in satisfactory agreement with the experimental results.

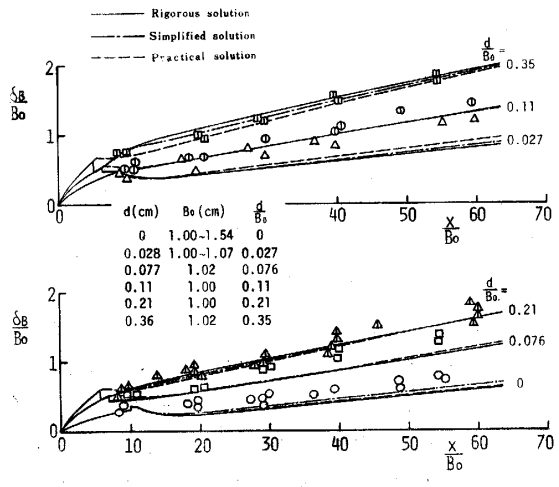

Fig. 17 Boundary layer growth in plane wall jets.

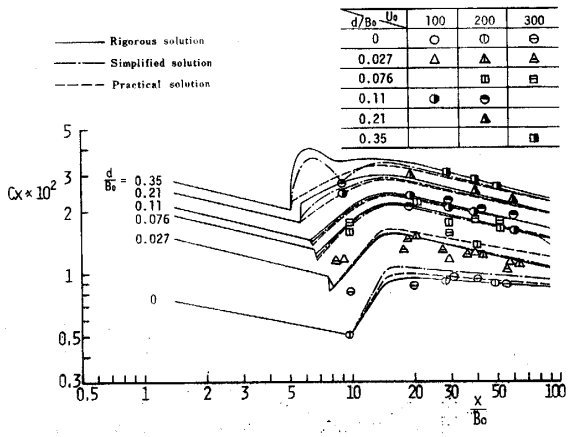

Fig. 18 Friction coefficient in plane wall jets.

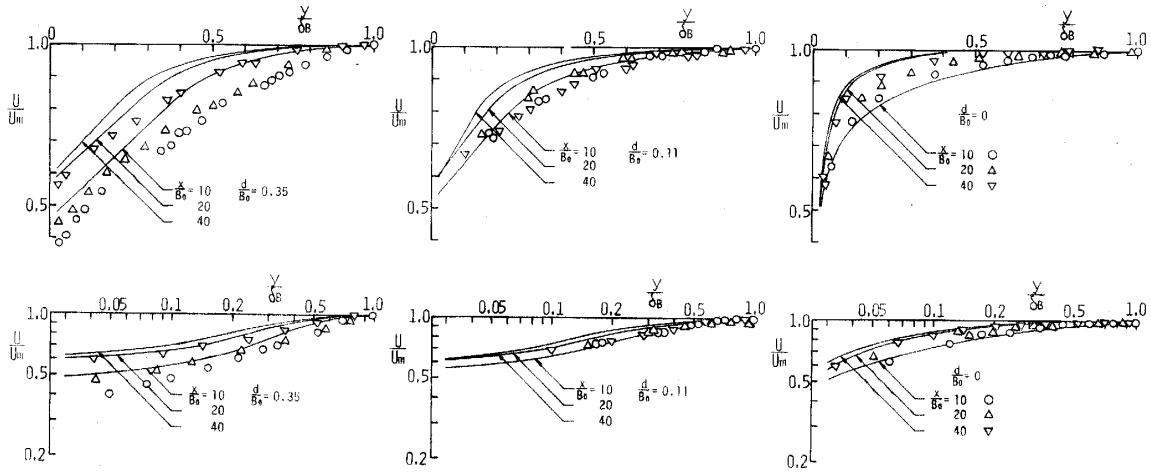

Fig. 19 Velocity profiles in plane wall jets.

6. The influence of water depth at downstream

We discussed on some characteristics of turbulent wall jet in the case that a downstream depth was entirely large in previous chapters, but practically, it is common that a downstream depth is comparatively shallow owing to hydraulic conditions at the downstream. In such case, the downstream depth changes spatially and therefore, it is impossible to neglect a pressure term in the equation of motion. Considering this effect, we did a few experiments changing a downstream depth H and Froude number $U_0/\sqrt{gB_0}$ systematically.

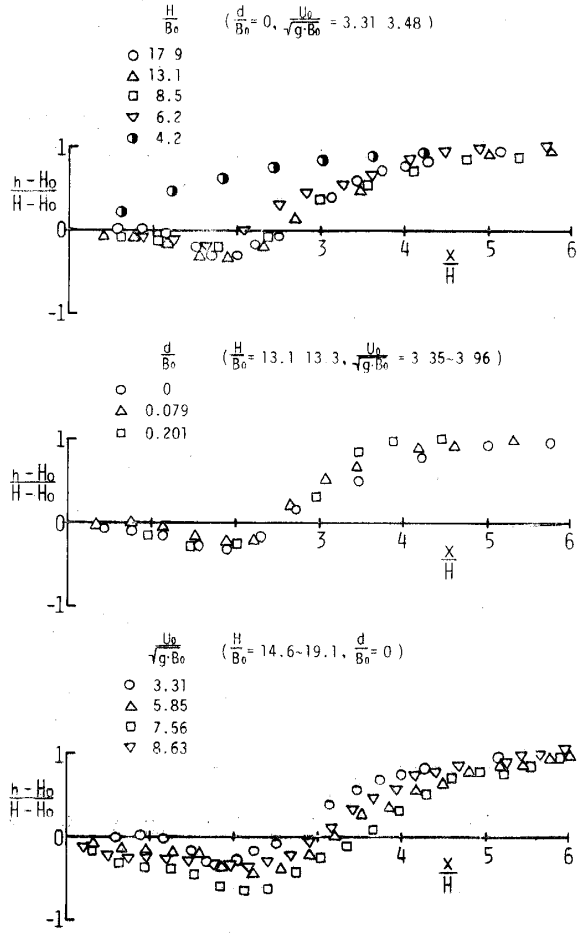

Fig. 20 The state of water surface downstream of a sluice.

Let mention on the limit to be able to apply the wall jet with these experiments.

Fig. 20 shows a part of the experimental results on the shape of the water surface measured by a static pressure tube, in where, H_0 denote a depth at the jet entrance section, H denote a depth at a far downstream and h is a depth in any section. When H/B_0 are larger than the conjugate depth with B_0, as was shown in this figure, the shape of the

water surface are almostly indicated by the normalized expression in spite of changing d/B_0, H/B_0, $U_0/\sqrt{gB_0}$.

Neglecting the wall resistance, the following equation is given from the theorem of momentum within the inspection section from the jet entrance section to a far downstream.

$$\frac{H_0}{H}=\sqrt{1+2\left(1-\frac{H}{B_0}\right)\frac{U_0^2}{gB_0}\Big/\left(\frac{H}{B_0}\right)^3} \qquad \cdots\cdots\cdots(42)$$

If $H_0=B_0$ in this equation, the relation of the conjugate depth are given, where a hydraulic jump begins at the jet entrance section.

The calculated results of $(H-H_0)/H$ which are corresponds to changing quantity of the depth and $(H-H_0)/B_0$ which are corresponds to the gradient of water surface, and the experimental results are shown in Fig. (21), (22).

The curves of H/B_0, U_0/gB_0 in Fig. (21), (22) express the relation that a hydraulic jump occur at the jet entrance section. Therefore, in the zone of the right side of this curves, a jet flow exposed at the downstream.

The calculated and experimental results on the change of maximum velocity and the growth of the boundary layer are shown in Fig. 23, 24 respectively. In these figure, solid line indicate the result of the wall jet, and a line with symbol indicate the limits for applicating the wall jet. Then the value of x/B_0 are almostly twice as large as

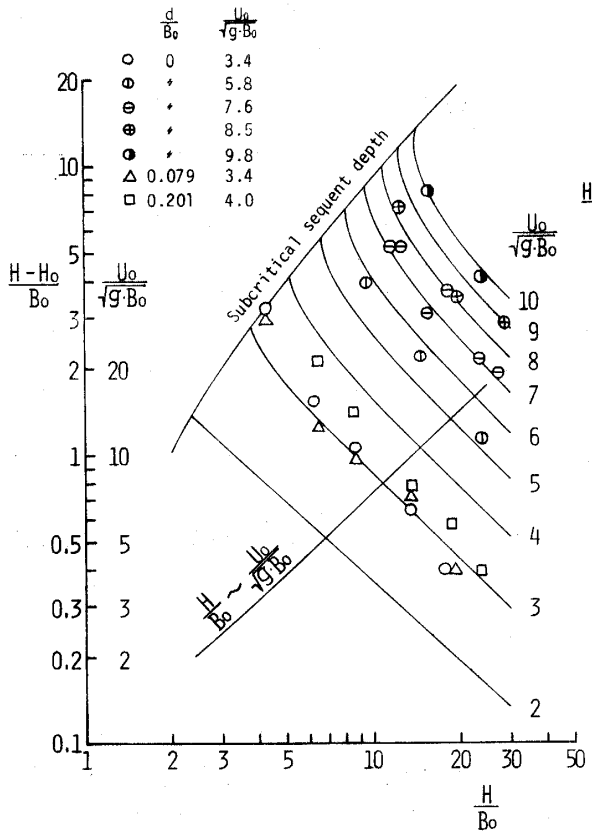

Fig. 21 Corelation of $(H-H_0)/B_0$ and H/B.

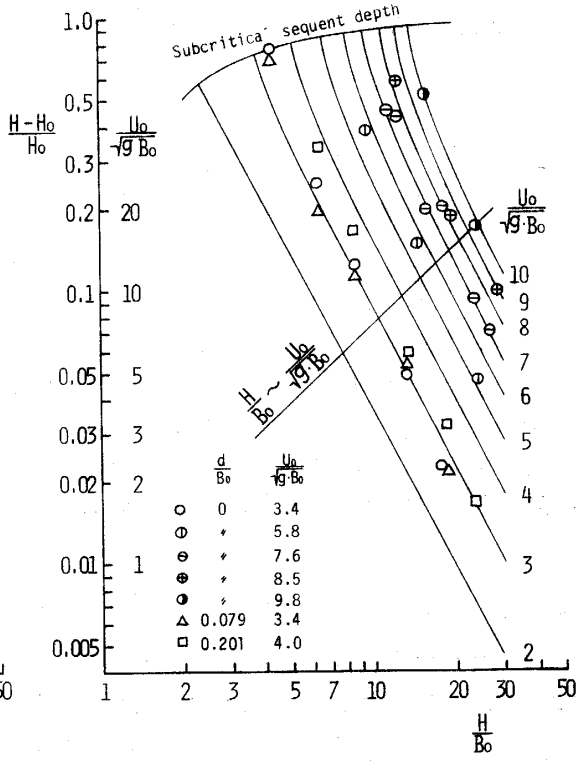

Fig. 22 Corelation of $(H-H_0)/H_0$ and H/B_0.

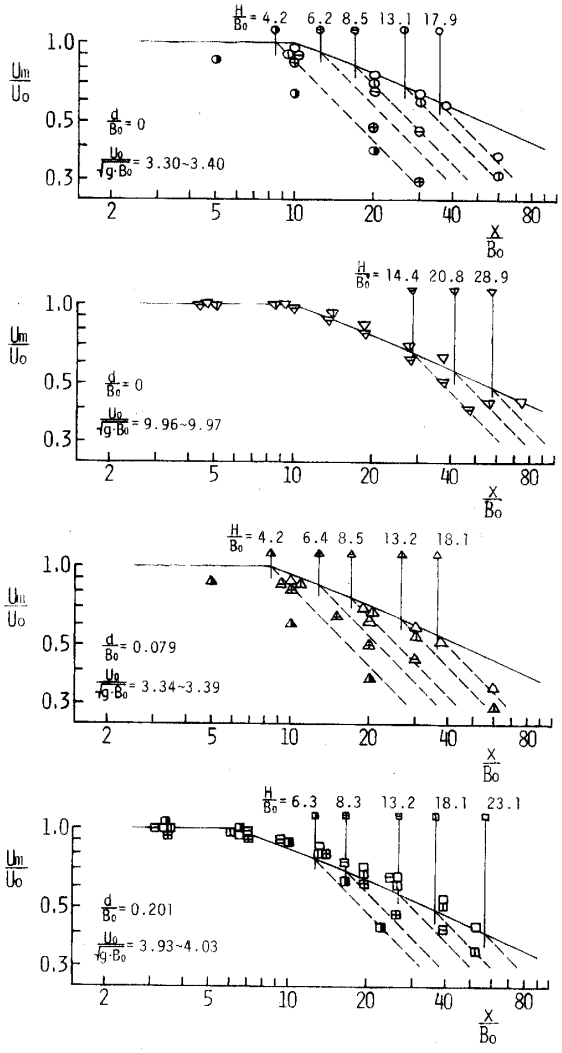

Fig. 23 Decay of the maximum velocity in the case of considering influences of downstream current depth.

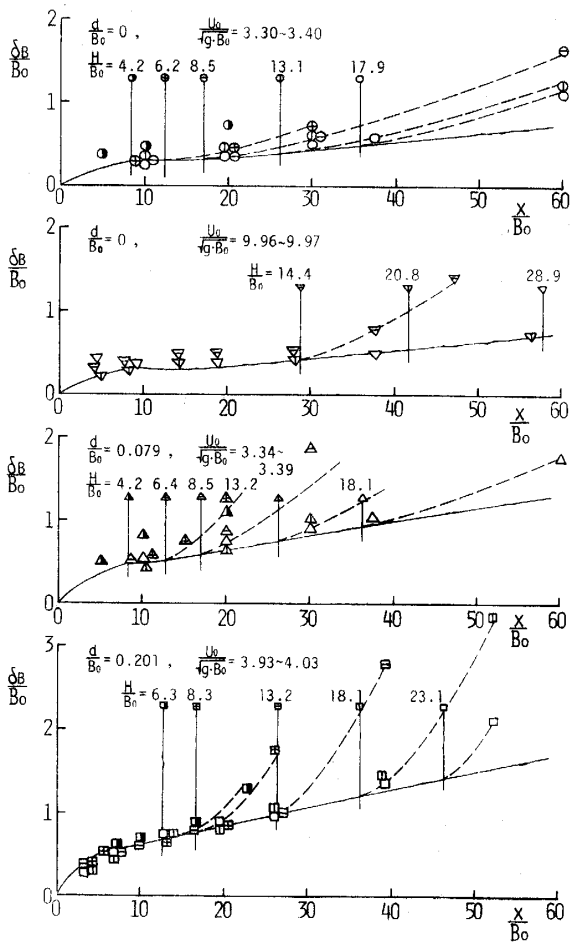

Fig. 24 Boundary layer growth in the case of considering influences of downstream current depth.

H/B_0. And, the point of $x/H=2$ almost coincide with the point at where the gradient of water surface change conversely on the shape of water surface in Fig. 18. It is possible to mention a marked trend that the exfloliation of flow in the boundary layer on condition of $dp/dx>0$ occur.

Judging from the above synthetically, we can consider that the limit of the extent applicated the results of the wall jet are $x/H<2$.

Conclusion

A summary of the experimental conclusion on the wall jet which diffuse along the smooth and rough wall surface and the theoretical conclusion on the velocity distribution in boundary layer considered the turbulence of main flow is the following.

It is possible to mention that the ratio of the main flow and the boundary layer

flow δ_B/δ_0 or the velocity distribution in the boundary layer change with the location gradually and the larger relative wall surface roughness is the larger ratio of the changes, accordingly, it is impossible to apply a similarity law of velocity distribution to the whole wall jet flow fields.

The diffusional characteristics in the main flow, which displays the change of U_m/U_0, δ_0/B_0 as same as on a free jet, can be indicated by eqn. (3), which denote the velocity distribution, rewrote the solution of Görtler by δ_0. And it is appeared that the coefficient of mixing length is constant in the field of jet like flow but, those values are about a half value of the free jet. The characteristics of the maximum velocity in the zone of established flow are explained by eqn. (9) which denotes the development boundary layer in the zone of established flow, and it is possible to apply the laws of momentum conservation to the flow field in the zone of establishment flow.

It is clarified that an exponential or logarithmic low of the velocity distribution and wall resistance can't apply to the development of boundary layer.

We could classify boundary layer into three layers that were a viscous sublayer in which the fluid viscosity dominated only, a turbulent sublayer in which a turbulent flow field owing to the wall roughness are build up, and an inner layer in which the diffusion of turbulent of the main flow are recognized, and introduce three equations of velocity distribution, which were eqns. (30), (39), (40), corresponding to each sublayer or layer, which coincide with Prandtl-Karman's logarithmic law in a special case.

Furthermore, we could confirm that both calculation results on the development of boundary layer and the wall resistance coefficient by the law of the velocity distribution, suggested by the author, consisted with the experimental conclusions fairly, considering the characteristics of the main flow in the experimental measurement. Similarly a good agreement between the calculation and the experiment on the velocity profile in the boundary layer exists under consideration of the experimental measurement errors. Therefore, it is possible to mention that the author's assumptions introduced in the process of inducement of the equations is almostly right.

Lastly, we could clarify that the limit of the application of the wall jet was in the range which the flowing length along downstream was smaller than the two times length of the downstream depth. The experimental and theoretical conclusions will be sufficiently useful to give some basic key of studies on a scour limit, a local scour mechanism in a downstream flow of a sluice gate and a development of boundary layer under a turbulent flow on a rough wall.

Acknowledgement

The author would like to express his gratitude to Prof. T. Tsubaki of Kyushu University, for useful suggestions in carrying out this study, and Y. Kameda, K. Hayashi, R. Fukamitsu, N. Yamamoto, and I. Ogi of Yamaguchi University, for frequent and helpful discussion and co-operation in the process of the experiment and calculation.

References

1) Glauert, M. B.: The wall-jet, Jour, Fluid Mech., Vol. 1, Part 6, 1956.
2) Schwartz, W. H. and W. H. Cosart: The two-dimensional wall jet, Jour. Fluid Mech., Vol. **10**, Part 4, 1961.
3) Sigalla, A.: Measurement of skin friction in a plane turbulent wall jet, Jour. Ray. Aero. Soc., Vol. **62**, 1958.
4) Kapaeva, A. K.: Hydrauric jump over a smooth or rough bottom regard as a wall jet, Tras, Hydraulic Eng., Vol. **92**, 1970.
5) Y. Tsuchiya: Studies on the mechanism of the local scour downstream of an outlet, Rep. 12th Hyd., Conf, 1967.
6) Rajaratnam. N.: Hydraulic jump, Advanced in hydrao-science, Vol. **4**, 1967.
7) Eskinazi, S. and V. Kruka: Mixing of turbulent wall-jet in to free-stream, Proc. A.S.C.E., Vol. **88**, EM 2, 1962.
8) Kruka, V. and S. Eskinazi: The wall-jet in a moving stream, Jour. Fluid Mech., Vol. **20**, Part 4, 1964.
9) Tollmien, W.: Berechnung turbulenter Ausbreitung vorgrange, Z.A.M.M., Helt **6**, 1926.
10) Gortler, H.: Berechnung Von Aufgaben der freien Turbulentz auf Grund eines neuen Naherungsansatzes, Z.A.M.M., Heft **22**, 1942.
11) Schlichting, H.: Boundary layer theory, McGrow-Hill.
13) Townsend, A. A.: The structure of the turbulent boundary layer, Pro. Cambridge Phil. Soc., Vol. **47**, 1951.
12) Hinze, J. O.: Turbulence, Mcgrow-Hill.
14) M. Kurihara: Studies on the turbulent structure (III), R.I.F.E., Kyushyu University, Vol. **2**, Part 3, 1943. (in Japanese)
15) M. Kurihara: Pipe resitsance coefficient in the transition region (I), R.I.F.E., Kyushyu University, Vol. **7**, Part 4, 1951. (in Japanese)
16) M. Kurihara: Pipe resistance coefficient in the transition region (II), R.I.F.E., Kyushyu University, Vol. **7**, Part 4, 1951. (in Japanese)